# $^{13}$C metabolic flux profiling of *Pichia pastoris* grown in aerobic batch cultures on glucose revealed high relative anabolic use of TCA cycle and limited incorporation of provided precursors of branched-chain amino acids

Meng Zhang[1], Xiao-Wei Yu[1], Yan Xu[1], Paula Jouhten[2], G. V. T. Swapna[3], Ralf W. Glaser[4], John F. Hunt[5], Gaetano T. Montelione[3,6], Hannu Maaheimo[7] and Thomas Szyperski[8]

1 School of Biotechnology and Key Laboratory of Industrial Biotechnology, Ministry of Education, Jiangnan University, Wuxi, China

2 European Molecular Biology Laboratory Heidelberg, Heidelberg, Germany

3 Center for Advanced Biotechnology and Medicine, Department of Molecular Biology and Biochemistry, Rutgers, The State University of New Jersey, Piscataway, NJ, USA

4 Institute of Biochemistry and Biophysics, Friedrich-Schiller-Universität, Jena, Germany

5 Department of Biological Sciences, Columbia University, New York, NY, USA

6 Department of Biochemistry and Molecular Biology, Robert Wood Johnson Medical School, Rutgers, The State University of New Jersey, Piscataway, NJ, USA

7 VTT Technical Research Centre of Finland Ltd, Espoo, Finland

8 Department of Chemistry, State University of New York at Buffalo, Buffalo, NY, USA

**Keywords**

$^{13}$C NMR, Metabolic Flux, Metabolite Transport, *Pichia pastoris*, *Komagatella phaffi*

Article type : Regular Paper

**Correspondence**

XW. Yu, Y. Xu, The Key Laboratory of Industrial Biotechnology, Ministry of Education, School of Biotechnology, State Key Laboratory of Food Science and Technology, Jiangnan University, Wuxi 214122, Jiangsu, China

Tel: +86 0510 85918201

Email: yxu@jiangnan.edu.cn, bioyuxw@jiangnan.edu.cn

T. Szyperski, Department of Chemistry, State University of New York at Buffalo, Buffalo, NY 14260, USA

Fax: +1 716 6453639

Tel: +1 716 6454309

E-mail: szypersk@buffalo.edu

**Running title:** Metabolic study of *P. pastoris* in batch cultures

**Abbreviations**

MC, mitochondrial carrier; BDF, biosynthetically directed fractional; NMR, nuclear magnetic resonance; MS, mass spectrometry; cyt, cytosolic; mt, mitochondrial; TCA, tricarboxylic acid; PEP, phosphoenolpyruvate; PPP, pentose phosphate pathway; PYR, pyruvate; 2OG, 2-oxoglutarate; OAA, oxaloacetate; FUM, fumarate; α-KB, α-ketobutyrate; α-KIV, α-ketoisovalerate; F6P, fructose-6-phosphate; G3P, glyceraldehyde-3-phosphate; X5P, xylulose-5-phosphate; E4P, erythrose-4-phosphate; S7P, sedoheptulose-7-phosphate; GCS, glycine cleavage system; SHMT, serine hydroxymethyltransferase; TA, transaldolase; TK, transketolase; HSQC, heteronuclear single quantum coherence. *Enzymes*: acetohydroxy acid isomeroreductase (EC 1.1.1.86), branched-chain-amino-acid aminotransferase (BCAT, EC 2.6.1.42), fumarase (EC 4.2.1.2), malic enzyme (EC 1.1.1.39/1.1.1.40), phosphoenolpyruvate carboxykinase (EC 4.1.1.49), pyruvate carboxylase (EC 6.4.1.1), pyruvate kinase (EC 2.7.1.40), L-serine hydroxymethyltransferase (EC 2.1.2.1), threonine aldolase (EC 4.1.2.5), threonine dehydratase (EC 4.3.1.19); transketolase (EC 2.2.1.1), transaldolase (EC 2.2.1.2).


## Abstract

Carbon metabolism of Crabtree negative yeast *Pichia pastoris* was profiled using $^{13}C$ NMR to delineate regulation during exponential growth and to study the import of two precursors for branched-chain amino acid biosynthesis, α-ketoisovalerate and α-ketobutyrate. Cells were grown in aerobic batch cultures containing (i) only glucose, (ii) glucose along with the precursors, or (iii) glucose and Val. The study provided the following new insights. First, $^{13}C$ flux ratio analyses of central metabolism reveal an unexpectedly high anaplerotic supply of the tricarboxylic acid cycle for a Crabtree negative yeast, and show that a substantial fraction of glucose catabolism proceeds through the pentose phosphate pathway. A comparison with previous flux ratio analyses for batch cultures of Crabtree negative *Pichia stipitis* and Crabtree positive *Saccharomyces cerevisiae* indicate that the overall regulation of central carbon metabolism in *P. pastoris* is intermediate in between *Pichia stipitis* and *Saccharomyces cerevisiae*. Second, excess α-ketoisovalerate in the medium is not transported into the cytoplasm indicating that *P. pastoris* lacks a suitable transporter. In contrast, excess Val is efficiently taken up and largely fulfills demands for both Val and Leu for protein synthesis. Third, excess α-ketobutyrate is transported into the mitochondria for Ile biosynthesis. However, the import does not efficiently inhibit the synthesis of α-ketobutyrate from pyruvate indicating that *P. pastoris* has not been optimized evolutionarily to take full advantage of this carbon source. These findings have direct implications for preparing uniformly $^{2}H$,$^{13}C$,$^{15}N$-labeled proteins containing protonated Ile, Val and Leu methyl groups in *P. pastoris* for NMR-based structural biology.


## Introduction

The yeast *Pichia pastoris*, recently classified as the new genus *Komagatella phaffii* [1, 2], is widely used for expression of recombinant proteins that require disulfide bond formation or glycosylation [3]. In spite of its outstanding importance for biotechnology and life sciences in general, however, the incomplete annotation of its genome [4, 5] and the lack of a model organism database, as they exist for *Escherichia coli* and *Saccharomyces cerevisiae*, impede research progress [6]. Experimental studies of *P. pastoris*' central carbon metabolism are likewise comparatively rare [7-16].

As a result, our knowledge of the physiological capabilities of *P. pastoris* is rather incomplete and additional metabolic studies are required. Earlier investigations of *P. pastoris* central carbon metabolism were exclusively performed using chemostat cultures [7, 8, 12-16] where growth is limited by glycerol and/or glucose supply. In contrast, catabolic fluxes are maximal during exponential growth in (fed-)batch cultures which are therefore often preferred in biotechnological industry [17]. In fact, significant flux ratio differences were reported for the yeast species *S. cerevisiae* [18] and *Pichia stipitis* [19] (recently classified as *Scheffersomyces stipitis* [2]) when comparing chemostat and batch cultures with glucose containing minimal media [19]. Moreover, Sola *et al.* [7] compared central carbon metabolism of *P. pastoris*, *P. stipitis* and *S. cerevisiae* grown in chemostat cultures and reported flux ratio differences between *P. pastoris* and the other two yeast species. Such comparisons are of interest to enhance our understanding of the suppression of respiration in the presence of excess glucose ('Crabtree effect') [20, 21]: in contrast to *P. pastoris* and *P. stipitis*, *S. cerevisiae* is Crabtree-positive.

For the earlier metabolic studies [7, 8, 12-16], biosynthetically directed fractional (BDF) $^{13}C$ labeling of proteinogenic amino acids was employed, which is accomplished with mixtures of uniformly $^{13}C$-labeled (typically 10%) and unlabeled carbon source molecules. BDF $^{13}C$-labeling corresponds to a carbon-carbon bond labeling approach and information on the catabolic breakage of carbon-carbon bonds is encoded in $^{13}C$–$^{13}C$ scalar coupling fine structures (in contrast to 'tracer' experiments, the enrichment with $^{13}C$ is uniform and does not encode metabolic information). BDF $^{13}C$-labeling of proteins was introduced in structural biology to obtain stereo-specific nuclear magnetic resonance (NMR) assignments for the methyl groups of Val and Leu [22, 23] by taking advantage of the stereo-specificity of the enzyme acetohydroxy acid isomer-reductase catalyzing the migration of the pro-S methyl group when the isopropyl moiety of Val and Leu is formed. Considering also earlier metabolic studies pursued with uniformly $^{13}C$-labeled metabolites (for a review, see [24]), BDF $^{13}C$ labeling of biomass and thus proteinogenic amino acids was then established [25] to profile bacterial central carbon metabolism [26-34] by use of NMR and later mass spectrometry (MS) (for reviews, see for example [16, 24, 35]). Subsequently, this approach was extended for eukaryotic cells, that is, for the yeast species *S. cerevisiae* [18, 36], *P. stipitis* [19], and *P. pastoris* [7, 8], the fungus *Trichoderma reesei* [37] and plant cells [38]. BDF $^{13}C$-labeling of proteinogenic amino acids allows to (i) validate and/or explore biosynthetic pathways for amino acids [39], (ii) confirm a biochemical reaction network of central carbon metabolism, and (iii) derive metabolic flux ratios [18, 25, 27], which can also be employed as experimental constraints for metabolic flux balancing analyses, *e.g.* [16, 27].

The biochemical reaction networks of central carbon metabolism previously derived for *P. pastoris* [7, 8] were recently extended into a genome-wide metabolic reconstruction [40]. This enables a suitable expansion of the central carbon 'core' network [7, 8] for future studies. Eukaryotic cells are compartmentalized and the localization of isoenzymes (*e.g.* [41]) for amino acid biosynthesis varies between different yeast species [42]. Furthermore, metabolites need to be transported across membranes, in particular the inner mitochondrial (mt) membrane. Such transport represents a critical feature which is not accurately captured in any current metabolic network model. In fact, our knowledge on the mitochondrial carriers (MCs) is quite limited: the genome of *S. cerevisiae* encodes 35 MCs but their functional annotation is incomplete [43]. Furthermore, at least some MCs exhibit remarkable 'promiscuity', that is, they have been shown to transport a variety of metabolites and it might well be that some metabolites are transported by more than one MC. As a result, the transport mechanisms of many metabolites are either only partially known or unknown [43]. The same holds for the regulation of the transporter, which may evidently play an important role for metabolic

regulation in general [43]. Notably, the MC subfamily for di-/tri-carboxylates and α-ketoacids is of particular importance for eukaryotic central carbon metabolism [43, 44].

In another vein, due to its high efficacy in expressing disulfide-containing and/or glycosylated proteins [3], *P. pastoris* also represents a valuable host organism for generating stable isotope labeled proteins for structural biological studies using NMR spectroscopy [45-51]. NMR signals broaden in proportion to the correlation time of the rotational reorientation of a protein molecule, primarily due to $^{1}H$ -$^{1}H$ and $^{1}H$-$^{13}C$ dipolar interactions. Hence, studies of high molecular weight systems (> ~ 30 kDa) require not only that the protein is uniformly $^{13}C$,$^{15}N$-labeled to enable $^{13}C$,$^{15}N$-resolved multi-dimensional NMR, but also that the protein is deuterated to eliminate a large fraction of the $^{1}H$ spins. To nonetheless allow the detection of the $^{13}C^{1}H_3$ NMR signals of Ile, Val, Leu residues, their methyl groups need to remain protonated in an otherwise deuterated background [52]. Such isotope labeling results in 'ILV-samples' and requires that two appropriately $^{13}C$-labeled and methyl protonated key intermediates of Ile, Val, Leu biosynthesis, that is, α-ketobutyrate (α-KB) and α-ketoisovalerate (α-KIV), both α-ketoacids, are added to a minimal medium in $^{2}H_2O$ containing uniformly $^{13}C$,$^{2}H$-labeled glucose as the sole carbon source [53]. For overexpression in *E. coli*, the protocol to generate ILV-samples is nowadays widely used. In contrast, attempts to generate ILV-samples for proteins overexpressed in *P. pastoris* were only partially successful for Ile, and largely failed for Leu and Val [54, 55]. Due to the incompleteness of our knowledge of *P. pastoris*' and yeast metabolism in general as explained above, these findings could only be partially rationalized.

We thus initiated the first NMR based BDF $^{13}C$-labeling study of *P. pastoris* central carbon metabolism in batch cultures containing glucose as the sole carbon source. While our investigation was in progress, an MS based $^{13}C$ metabolic flux analysis of *P. pastoris* grown in a batch culture was published [56]. This enabled valuable cross-validation of the information on flux distributions obtained independently from our study. Secondly, to shed new light on metabolite transport and to potentially support the improvement of protocols for production of ILV-samples, we performed a cost-effective comparative BDF $^{13}C$-labeling study with *P. pastoris* grown in a minimal medium containing 10% uniformly $^{13}C$-labeled glucose and 90% unlabeled glucose along with unlabeled α-KIV and/or α-KB, or unlabeled Val. Our study revealed new insights into flux distributions during exponential growth and transport of precursors of branched-chain amino acids in yeasts (Fig. 1).

## Results and Discussion

### Metabolic flux ratio analysis for *P. pastoris* grown in an aerobic batch culture containing solely glucose as a carbon source

Catabolic fluxes of central carbon metabolism are maximal during exponential growth in (fed-)batch cultures. Hence, their characterization is of high interest for understanding yeast metabolism and the improvement of biotechnological processes [17]. Following previously described protocols [7, 18, 19], $^{13}C$ metabolic flux ratio analyses were performed in duplicate for two cultures G-1 and G-2 of *P. pastoris* strain GS115 (Table 1) growing exponentially in aerobic batch cultures with minimal media containing glucose as the sole carbon source (the corresponding *f* values are provided, respectively, in Tables S1, S2 and S3). Table 2 provides the determined flux ratios along with (i) ratios previously reported for very similar batch cultures of *S. cerevisiae* [18] and *P. stipitis* [19], and (ii) ratios that could be calculated from the net fluxes obtained by Nie *et al.* [56] in an MS based $^{13}C$ flux analysis performed for *P. pastoris* cells of the same strain grown in a very similar batch culture. Fiaux *et al.*

[19] compared the ratios of *S. cerevisiae* and *P. stipitis* in detail. For the sake of clarity, the comparison of *P. pastoris* with the other yeast species follows the discussion of Fiaux *et al.*, and the biochemical reactions and corresponding enzymes are depicted in Fig. 1.

**(1)** The upper bound for the fraction of phosphoenolpyruvate (PEP) derived from the transketoloase (TK) reaction interconverting fructose-6-phosphate (F6P) and glyceraldehyde-3-phosphate (G3P) into xylulose-5-phosphate (X5P) and erythrose-4-phosphate (E4P) (Fig. 1; Table 2) are quite high for *P. pastoris* (34%) and *P. stipitis* (57%), while a much lower bound was obtained for *S. cerevisiae* (0-4%) (Fig. 2). These values indicate that for both *P. pastoris* and *P. stipitis* a substantial fraction of glucose catabolism proceeds through the pentose phosphate (PP) pathway while *S. cerevisiae* glucose catabolism is quite restricted to glycolysis (Crabtree effect, [20, 21]). Consistently, the *P. pastoris* flux balancing study of Nie *et al.* (see Fig. 6 in [56]) revealed that about 27% of PEP is synthesized *via* the PP pathway (Table 2).

**(2)** The fraction of mitochondrial (mt) oxaloacetate (mt-OAA) generated by carboxylation of pyruvate (PYR) by pyruvate carboxylase (Fig. 1) increases from *P. stipitis* (36%) to *P. pastoris* (59%), and to *S. cerevisiae* (76%) (Fig. 2; Table 2). The value obtained here for *P. pastoris* is close to the flux ratio (45%) calculated from the fluxes of Nie *et al.* (see Fig. 6 in [56]) and is in between *P. stipitis* and *P. pastoris*. This is likely due to the fact that cells in the study of Nie *et al.* were grown in a culture with intense aeration to ensure 'fully aerobic conditions'. Taken together, the employment of the TCA cycle to fulfill biosynthetic demands in Crabtree negative *P. pastoris* is intermediate between Crabtree negative *P. stipitis* and Crabtree positive *S. cerevisiae* (note that the high anaplerotic flux ratio reflects a repressed respiratory metabolism due to the Crabtree effect [20, 21]).

**(3)** Cytosolic (cyt) oxaloacetate (cyt-OAA) is synthesized primarily from PEP (by action of pyruvate kinase and then pyruvate carboxylase) in *P. pastoris* (74%), which is in between the corresponding fractions in *S. cerevisae* 88-100%) and *P. stipitis* (41%).

**(4)** The fraction of cyt-OAA that was at least once reversibly interconverted to fumarate (FUM) by fumarase (Fig. 1) is much lower in both *P. pastoris* and *S. cerevisae* (0-4%) than in *P. stipitis* (24%), and the fraction of mt-OAA reversibly interconverted to FUM increases in the order *S. cerevisiae* (35%), *P. pastoris* (52%) and *P. stipitis* (58 %) (Fig. 2; Table 2).

**(5)** The fraction of mt-PYR synthesized from mt-malate by the malic enzyme (Fig. 1) is very low in *P. pastoris* and *P. stipitis* (< 6%), but significant in *S. cerevisiae* (25-30%) (Fig. 2; Table 2).

In contrast to these pronounced differences, similar flux ratio values are observed for all three yeast species for (i) the gluconeogenetic interconversion of cyt-OAA to cyt-PEP by PEP carboxykinase (Fig. 1) (< 5%), (ii) ranges of ratios of other fluxes associated within the PP pathway (Fig. 1; Table 2), and, (iii) the fractions of Ser and Gly which were reversibly cleaved by Ser hydroxymethyltransferase (SHMT) and the Gly cleavage system (GCS). This indicates similar regulation of $C_1$-metabolism.

Overall, the flux ratio analysis revealed that the three yeast species show distinctly different regulation of central carbon metabolism (Fig. 1) when glucose is provided in excess as the sole carbon source in an aerobic batch culture (Fig. 2). In particular, the two Crabtree-negative yeasts *P. stipitis* and *P. pastoris* do not form a 'group' which can readily be distinguished from Crabtree-positive *S.*

*cerevisiae*. While the predominant use of the TCA cycle to generate intermediates for biosynthesis is expected for *S. cerevisiae* when respiration is repressed, the high anabolic use of the TCA cycle in Crabtree negative *P. pastoris* is unexpected and in stark contrast to *P. stipitis*. Furthermore, the anaplerotic supply of the TCA cycle is likewise significantly lower in *P. pastoris* glucose-limited chemostat cultures (at a dilution rate of 0.16 $h^{-1}$) [7] (40%), suggesting that *P. pastoris* indeed suppresses respiration when glucose is supplied in excess in batch cultures.

### Comparative study of *P. pastoris* grown in an aerobic batch culture containing glucose along with α-KIV and/or α-KB, or Val as carbon sources

For disulfide-containing and/or glycosylated proteins [3] *P. pastoris* represents an attractive host organism for expressing stable isotope labeled proteins for studies using NMR spectroscopy [45-51]. Hence, to evaluate the suitability of *P. pastoris* for the production of ILV-samples, we initially tested if α-KIV and/or α-KB are taken up by the cells to a significant extent during the exponential growth phase: varying amounts of unlabeled precursor (between 0.1 and 1 g/L of each precursor) were added to the medium containing the uniformly $^{13}$C-labeled glucose (set 1 of cultures, GBI-1 to GBI-4 in Table 1). There are two key advantages of such 'unlabeling' experiments. First, no expenses are incurred for the $^{13}$C-labeled precursors. Second, the calculation of flux ratios does not rely on labeling patterns detected for Val, Leu and Ile. Hence, central carbon metabolism can be profiled simultaneously as long as the degradation of the unlabeled amino acids can be neglected. Overall, such unlabeling experiments are thus cost effective.

In order to detect a reduction of the degree of $^{13}$C labeling ('unlabeling') of Ile, Val and Leu arising from the import of the unlabeled precursors and subsequent biosynthesis of the branched chain amino acids from these precursors, the signals of Ile, Val and Leu methyl groups were integrated in the 2D [$^{13}$C,$^{1}$H] heteronuclear single quantum coherence (HSQC) spectra. Subsequently, the peak volumes measured in each of the spectra were divided by the respective volume of the methyl group of Met. The methyl group of Met is a suitable internal standard since neither the degree of $^{13}$C labeling of the Met methyl group nor the relative abundance of Met in the biomass is affected when the unlabeled precursors are taken up. First, the methyl group of Met originates from C1 metabolism and the precursors are not interconverted into Ser or Gly (which supply $C_1$-units when cells are grown in media with excess glucose). Second, even potential degradation of Ile, Val and Leu *via* the Ehrlich pathway [57] results in metabolites which are excreted and likewise not connected to C1 metabolism and the transfer of a methyl group to synthesize Met.

Analysis of the thus obtained normalized volumes of the methyl group signals of Ile and Val/Leu showed that, respectively, incorporation of α-KIV in Val and Leu was not detected while a rather small fraction of α-KB was used for Ile biosynthesis (degree of $^{13}C^{\delta 1}$ unlabeling: ~15%). These findings were confirmed by the $f^{(1)}$ and $f^{(2)}$ values registered for the Ile, Val and Leu methyl groups (note that unlabeling leads to a decrease of $f^{(2)}$ values because $f^{(2)} \approx 0$ at natural $^{13}$C abundance). Furthermore, the flux ratios obtained for GBI-1 to GBI-4 (data not shown) were virtually identical as those obtained for G-1 with glucose as the sole carbon source (left-most ratio in Table 2). This finding indicates that regulation of central carbon metabolism was hardly affected, and that exponential growth is not impeded by the availability of α-KB and α-KIV in the media.

While our study was in progress, Clark *et al*. [55] published an investigation focusing on the preparation of ILV-samples in *P. pastoris*. Consistent with our findings, Clark *et al.* reported that $^{13}$C-labeled

α-KIV in the medium does not result in the labeling of Val and Leu residues in an overexpressed target protein. However, it was observed that the presence of $^{13}$C-labeled α-KB in the media resulted in ~50% labeling of Ile residues. Very similar results were previously obtained by Miyazawa-Onami *et al.* [54] for ILV-sample preparation using the yeast species *Kluyveromyces lactis*. In addition, they reported that the availability of uniformly $^{13}$C-labeled Val in the media results in a virtually complete labeling of both Val and Leu residues in the overexpressed protein.

To further investigate how biosynthesis of branched chain amino acids is affected by the presence of

α-KB and Val in glucose containing growth media, we prepared two additional sets of cultures (Table 1). For set 2 (G-2, GV-2, GB-2 in Table 1), cells were grown to the end of the mid-exponential growth phase before they were harvested, while for set 3 (G-3, GV-3, GB-3 in Table 1), cells were grown until the stationary phase was reached. Fig. 3 provides the growth curves ($OD_{600}$ *versus* time), demonstrating that neither the addition of Val nor α-KB affects growth rates significantly. Fig. 4 shows the consumption of carbon source molecules (concentrations *versus* time) for all six cultures. The data reveal that a significant fraction of Val and α-KB in the media was taken up (~10% and ~40-50% after 7 and 15 h, respectively).

Inspection of normalized Val methyl group 2D [$^{13}$C,$^{1}$H] HSQC signal volumes (Fig. 5A) reveal (i) that Val is imported into cells to a significant extent during the exponential growth phase and used for protein synthesis, and (ii) that it is used nearly exclusively for protein synthesis once cell growth approaches the stationary phase (Fig. 4): the degree of Val methyl $^{13}$C unlabeling is ~45% for the GV-2 (set 2) and ~75% for GV-3 (set 3) cultures. Inspection of Fig. 3 reveals that more than 50% of the biomass of set 3 cultures is generated during the first 7 hours of exponential growth (as for set 2 cultures). Hence, the increase of the degree of unlabeling from 45% to 75% indicates that nearly all of the Val incorporated in the late exponential or stationary phase originates from the Val in the medium. Furthermore, nearly the same degrees of unlabeling are registered for Leu (Fig. 5B). This indicates that Val is efficiently converted into α-KIV for Leu biosynthesis (Fig. 1) which is in line with the recent discovery [42] that the only branched-chain-amino-acid aminotransferase (BCAT; http://www.ebi.ac.uk/interpro/protein/C4R7A4) of *P. pastoris* is located in the cytosol (note that enzymes for Leu biosynthesis downstream of BCAT are also located in the cytosol) (Fig. 1). Hence, the fact that α-KIV is not efficiently metabolized by *P. pastoris* (cultures GBI-1 to GBI-4, and study of Clark et al. [55]) leads to the conclusion that *P. pastoris* lacks a suitable system to transport α-KIV from the medium into the cytosol (Fig. 1).

The import of α-KB into cells and mitochondria was confirmed for the GB-2 (set 2) and GB-3 (set 3) cultures. The degrees of $^{13}$C unlabeling measured for the Ile $\delta^1$-methyl group (Fig. 5C) is ~10% for GB-2 and ~40% for GB-3. Notably, these values are significantly lower than those observed for Val and Leu methyl groups when Val is provided in the medium (see above). Hence, the import of α-KB does not effectively inhibit α-KB biosynthesis in the mitochondria, that is, in spite of the high abundance in the medium cells continue to synthesize α-KB. Interestingly, Clark *et al.* [55] found that a somewhat larger fraction of labeled Ile residues (~50%) was incorporated into an overexpressed protein when labeled α-KB is provided in the medium. This difference may indicate that a larger

fraction of α-KB is consumed when protein overexpression is induced and the demand of Ile for protein biosynthesis increases.

Since Val, Leu and Ile are not degraded to generate precursors for biosynthesis of other amino acids as long as cells grow exponentially on a media containing glucose (e.g. [58]), we performed flux ratio analyses for cultures GV-2 and GB-2 (Table 1). Virtually the same ratios were obtained as for G-1 containing only glucose (Table 3) (Tables S6 and S8 provide the corresponding *f* values). This demonstrates that the regulation of central carbon metabolism is at most minimally affected by the presence of either Val or α-KB in the growth medium. In particular, a reduced demand for the precursors required for Val biosynthesis (given that Val is available in the medium) apparently does not trigger any significant redistribution of fluxes.

Finally, the differences of *f* values obtained for the set 2 culture G-2 and for the set 3 cultures G-3, GV-3 and GB-3 (Table 1), readily apparent by inspection of the corresponding $^{13}C$ scalar coupling fine structures (Fig. 6), suggested several hypotheses regarding changes in the metabolic regulation when cell growth reaches the stationary phase. First, a reduced fraction of intact $C^{\alpha}$-$C^{\beta}$ bonds [corresponding to $f^{(2)} + f^{(3)}$ shown in Fig. 6] observed for the set 3 cultures (G-3, GV-3, and GB-3) for Glu $C^{\alpha}$ compared to Pro $C^{\alpha}$ suggests that protein turnover becomes important for the supply of the TCA cycle in the stationary phase. Protein degradation releases Glu which is deaminated to 2-oxoglutarate (2OG) entering the TCA cycle. Newly synthesized protein contains Glu with a reduced fraction of intact $C^{\alpha}$-$C^{\beta}$ bonds because a full cycle of the TCA cycle yields $C^{\alpha}$-$C^{\beta}$ bonds in which the two carbon atoms originate from two source molecules of glucose. In contrast, Pro degradation (a two reaction pathway) to Glu is suppressed in the presence of ammonium in *S. cerevisiae* [58]. Like for Glu, Asp can be interconverted to OAA through transamination and enters to TCA cycle. This likewise reduces the fraction of intact $C^{\alpha}$-$C^{\beta}$ bonds because this bond is newly formed during each cycle. Accordingly, a reduced fraction of intact $C^{\alpha}$-$C^{\beta}$ bonds is observed for Asp $C^{\alpha}$ when compared with Met $C^{\alpha}$. Note that, upon degradation, the carbon skeleton of Met does not 'return' to central metabolism. Instead, the Ehrlich pathway in *S. cerevisiae* [57] yields metabolites which are excreted. Second, a reduced fraction of intact $C^{\alpha}$-$C^{\beta}$ bonds in Ala $C^{\alpha}$ (originating from mt-PYR) when comparing G-2 with the set 3 cultures indicates that malic enzyme, which catalyzes the synthesis of mt-PYR from malate (Fig. 1), becomes more important during stationary phase. PYR which is synthesized from malate exhibits a reduced fraction of intact bonds due to the action of the TCA cycle which reduces the fraction of intact C2-C3 bonds in malate. Third, a somewhat reduced fraction of intact $C^{\alpha}$-$C^{\beta}$ bonds in Phe $C^{\alpha}$ and Tyr $C^{\alpha}$ (originating from PEP) when comparing G-2 with the set 3 cultures suggests that the same holds for PEP carboxykinase, which catalyzes the generation of PEP from OAA (Fig. 1). Fourth, a reduced fraction of intact $C^{\alpha}$-$C^{\beta}$ bonds in Ser $C^{\beta}$ [corresponding to $f^{(2)}$ shown in Fig. 6] when comparing G-2 with the set 3 cultures reflects an alteration of $C_1$ metabolism during stationary phase. Fifth, a reduced fraction of intact $C^{\alpha}$-$C^{\beta}$ bonds in Thr $C^{\alpha}$ observed when comparing G-2 with set 3 cultures indicates a modulation of the role of Thr aldolase, which interconverts Thr into Gly and acetaldehyde.

To conclude, we conducted the first $^{13}C$ NMR based flux ratio analysis for *P. pastoris* cells grown exponentially in aerobic batch cultures containing glucose as the sole carbon source. The corresponding *f* values (Supporting Information) are thus available for researchers to benchmark future *in silico* metabolic studies (e.g. *f* values can augment systems of flux balancing equation [32]).

The comparably high relative anabolic use of the TCA cycle in Crabtree negative *P. pastoris* was most unexpected. Comparison of the flux ratios with those of *P. stipitis* and *S. cerevisiae* revealed distinct differences between the three yeast species and indicated that their physiological capabilities vary significantly. Importantly, metabolic regulation in Crabtree-negative *P. pastoris* is apparently not more similar to *P. stipitis*, which is also Crabtree-negative, than to Crabtree-positive *S. cerevisiae* [7]. Future studies, such as the systems biology study recently conducted for *P. stipitis* [20], potentially combined with isotopically non-stationary metabolic flux analyses [59], will be required to understand why *P. pastoris*' comparably low respiratory use of the TCA cycle in aerobic batch cultures is intermediate between Crabtree-negative *P. stipitis* and Crabtree-positive *S. cerevisiae*.

Furthermore, our investigation of how *P. pastoris* metabolizes Val and two key precursors for the biosynthesis of branched chain amino acids resulted in new insights regarding metabolite transport. First, the apparent lack of an α-KIV transporter in the plasma membrane suggests that no evolutionary pressure existed in nature to select for such a transporter. It is tempting to speculate that this is because α-KIV is rarely present in a natural environment as a carbon source. In contrast, Val is efficiently taken up by amino acid transporter systems and subsequently deamidated to α-KIV by cytosolic BCAT in order to satisfy also most of the demand for Leu biosynthesis. Second, α-KB transporters are present in the plasma and inner mitochondrial membranes but α-KB taken up by the cells does not inhibit synthesis from Thr. Considering that α-KB is likewise a carbon source rarely encountered in a natural environment, it might thus be that the enabling transporter systems are members of the promiscuous subfamily for di-/tri-carboxylates and α-ketoacid transporters (see introduction), which have not been evolutionarily optimized to handle α-KB.

Finally, our study identified two major bottlenecks for the preparation of ILV-samples for structural biology in *P. pastoris*. The lack of α-KIV transport into the cytoplasma represents the first one. Although addition of methyl protonated, $^{13}C$,$^{2}H$-labeled Val to the medium can circumvent this bottleneck, it appears desirable to create a *P. pastoris* strain with a suitably modified existing, or a newly engineered α-KIV transporter. The low efficiency of α-KB transport into the mitochondria represents the second bottleneck, which could be removed by the same strategy targeting transport across plasma and mitochondrial membrane. Alternatively, the enzyme threonine dehydratase interconverting Thr into α-KB could be knocked out in order to generate a *P. pastoris* strain that is auxotrophic for α-KB, which then needs to be supplied in the medium.

## Materials and Methods

### Cultures and biosynthetically directed fractional $^{13}C$ labeling

*Preparation of 'overnight cultures'. P. pastoris* strain GS115 was purchased from Invitrogen BV (Invitrogen BV, The Netherlands). Cells were first grown overnight at 30 °C in 40 mL of a yeast minimal medium (100 mM potassium phosphate, pH 6.0) containing glucose (5 g/L), $(NH_4)_2SO_4$ (5 g/L), YNB (VWR, Radnor, USA) solution (3.5 g/L; YNB without amino acids and ammonium sulfate), biotin (0.4 mg/L), in 500 mL baffled shake flasks using a shaker at 220 r.p.m until $OD_{600}$ reached 2-3. Cells were then centrifuged (3,000 r.p.m, 5 min) and resuspended in about 1 mL of de-ionized and sterilized water.

*Batch cultures.* Eleven cultures were performed in three different sets (Table 1). For eight of these cultures, cells were grown exponentially until the $OD_{600}$ reached ~2 after 6-7 hours (sets 1 and 2; Table 1), and for three cultures cells were grown until the stationary phase was reached ($OD_{600}$ > 3) after 15 hours (set 3; Table 1). The minimal media, as described for the overnight cultures, contained either only a mixture of 10% (w/w) U-$^{13}$C labeled (CIL Inc., USA) and 90% unlabeled glucose (5 g/L) ['G-1, G-2, G-3' in Table 1], or (a) in addition 0.1, 0.2, 0.5, or 1.0 g/L of unlabeled α-KB (Sigma Aldrich Inc., USA) and the same amount of unlabeled α-KIV (Sigma Aldrich Inc., USA) ['GBI-1' to 'GBI-4' of set 1; Table 1 ], (b) in addition 0.5 g/L unlabeled Val (Sinopharm Group Ltd., China) ['GV-2', 'GV-3' of sets 2 and 3; Table 1], (c) in addition 0.5 g/L of unlabeled α-KB ['GB-2', 'GB-3' of sets 2 and 3; Table 1]. For each culture, about 200 µL of the overnight culture were used to inoculate 40 mL of the minimal medium in 500 mL baffled shake flasks. Cultures were performed as described for the overnight cultures. The cells were harvested by centrifugation at 4,800 r.p.m for 10 min. Subsequently, the pellet was resuspended in Tris/HCl (20 mM, pH 7.6) and centrifuged again at 4,000 r.p.m. for 10 min. The thus obtained pellet was vacuum-dried to constant mass. 20 mg of the dried biomass were resuspended in 1 mL of 6 M HCl and hydrolysed for 24 h in a sealed glass tube at 110 °C. Finally, the solutions were ultra-filtered (0.22 µm) and lyophilized.

To monitor cell growth, $OD_{600}$ readings were taken during the cultures of sets 2 and 3, and to monitor the consumption of carbon source molecules during these cultures, 1D $^{1}$H NMR spectra (measurement time: 6 min each) were recorded using a Bruker Avance 400 MHz spectrometer, and processed and analyzed using Topspin 3.5 (Bruker Inc.). At defined time points (Figs. 2, 3) an aliquot of 1 mL was taken from the cultures. 200 µL were used to measure $OD_{600}$, while cells were removed from the remaining 800 µL by centrifugation and ultrafiltration (0.22 µm). Subsequently, 500 µL of the cell-free medium was lyophilized, redissolved in $^{2}H_2O$ and used for NMR data acquisition after addition of 10 mM 4,4-dimethyl-4-silapentane-1-sulfonate sodium salt (DSS).

**NMR spectroscopy**

The dried hydrolyzed biomass samples resulting from the eleven cultures (Table 1) were dissolved in 0.1 M $^{2}$HCl in $^{2}H_2O$ with 10 mM DSS. 2D [$^{13}$C,$^{1}$H] HSQC spectra [60] were acquired as described [23, 25, 27, 30] at 25 °C. For the samples of set 1, an aliphatic 2D [$^{13}$C,$^{1}$H] HSQC spectrum was acquired (in 16 hours) using a Bruker Avance 600 MHz spectrometer equipped with a TXI 1.7 mm micro-cryogenic probe (the aromatic signals were aliased). For the samples of sets 2 and 3, both aliphatic (7 hours) and aromatic 2D [$^{13}$C,$^{1}$H] HSQC spectra (4 hours) were acquired using a Bruker Avance 600 MHz spectrometer equipped with a TCI cryogenic probe. For the samples of cultures G-2 and G-3 (Table 1), aliphatic (6.5 hours) and aromatic 2D [$^{13}$C,$^{1}$H] HSQC spectra (6.5 hours) were also acquired using a Bruker Avance 850 MHz spectrometer equipped with a QCI cryogenic probe. High-quality 1D $^{1}$H NMR spectra were acquired to determine the degree of $^{13}$C-labeling, $p_l$, from integration of well resolved $^{13}$C satellites [25], yielding $p_l$ = 0.113 which is in close agreement with the value expected from the composition of the minimal medium. All 2D spectra were processed using the programs NMRPipe and NMRDraw [61].

**Data analysis**

$^{13}C$ scalar fine structures were integrated as described [29] and an EXCEL sheet was set up to calculate the relative abundances, *f*, of intact carbon fragments arising from a single source molecule of glucose [25, 26]. For independent validation, *f* values were calculated using Matlab R2016b v.9.1. This implementation also allowed 'suppression' of slightly negative *f* values, which were set to zero and constrained the re-calculation of non-zero *f* values. The biochemical reaction network was assumed to operate in a quasi-steady state as described previously [7, 8, 18, 19, 27, 28, 34] and the *f*-values were used to calculate flux ratios in both EXCEL and Matlab following refs [7, 18, 25, 27, 36]. As described [24, 25] (Fig. 6), $f^{(1)}$ represents the fraction of molecules with the observed carbon atom and its neighboring carbons originating from different source molecules of glucose, $f^{(2)}$ the fraction of molecules in which the observed carbon atom and at least one neighboring carbon originates from the same source molecule. For a central carbon in a $C_3$ fragment which exhibits different $^{13}C$-$^{13}C$ scalar coupling constants with the two attached carbons, $f^{(2)}$ represents the fraction of molecules for which the central carbon and the carbon with the smaller coupling come from the same source molecule, while $f^{(2*)}$ is used if the carbon with the larger coupling comes from the same source molecule as the observed carbon. $f^{(3)}$ denotes the fraction of molecules in which the observed carbon atom and both neighbours in the $C_3$ fragment originate from the same glucose molecule. The *f* values determined for the present study are provided as Tables S1 to S9 in the Supporting Information.

## Acknowledgments

Financial support from the High-end Foreign Experts Recruitment Program (GDW20123200113), NSFC (31671799), Six Talent Peaks Project in Jiangsu Province (NY-010), 333 Project in Jiangsu Province (BRA2015316), and the 111 Project (111-2-06) are greatly appreciated. NMR instrumentation at Rutgers University used in this work was supported in part by NIH grant 1S10OD018207. G.T.M. is supported in part by the Jerome and Lorraine Aresty Chair Endowment. We thank Dr. Dorothee Barth for helpful comments on the Matlab implementations.

## Author Contributions

M.Z., XW.Y, Y.X., J.F.H., G.T.M., T.S. planned experiments, M.Z., G.V.T.S., H.M. performed experiments, M.Z., H.M., P.J., R.W.G., T.S. analyzed data, and all authors wrote the paper.

## Supporting Information

Tables with *f* values obtained for the batch cultivations of Table 1.
Table S1: average of *f* values obtained for G-1, GBI-1, GBI-2, GBI-3, GBI-4 (set 1) [600 MHz]
Table S2: *f* values obtained for G-2 [600 MHz]
Table S3: *f* values obtained for G-2 [850 MHz]
Table S4: *f* values obtained for G-3 [600 MHz]
Table S5: *f* values obtained for G-3 [850 MHz]
Table S6: *f* values obtained for GV-2 [600 MHz]
Table S7: *f* values obtained for GV-3 [600 MHz]
Table S8: *f* values obtained for GB-2 [600 MHz]
Table S9: *f* values obtained for GB-3 [600 MHz]

## References


1. Yamada, Y., Matsuda, M., Maeda, K. & Mikata, K. (1995) The phylogenetic relationships of methanol-assimilating yeasts based on the partial sequences of 18S and 26S ribosomal RNAs: the proposal of Komagataella gen. nov. (Saccharomycetaceae), *Bioscience, biotechnology, and biochemistry.* **59**, 439-44.
2. Kurtzman, C. P., Fell, J. W. & Boekhout, T. (2011) The Yeasts A Taxonomic Study in pp. 2354 p., Elsevier Science & Technology Books, San Diego.
3. Cregg, J. M., Tolstorukov, I., Kusari, A., Sunga, J., Madden, K. & Chappell, T. (2009) Expression in the yeast Pichia pastoris, *Methods in enzymology.* **463**, 169-89.
4. Mattanovich, D., Callewaert, N., Rouze, P., Lin, Y. C., Graf, A., Redl, A., Tiels, P., Gasser, B. & De Schutter, K. (2009) Open access to sequence: browsing the Pichia pastoris genome, *Microbial cell factories.* **8**, 53.
5. Valli, M., Tatto, N. E., Peymann, A., Gruber, C., Landes, N., Ekker, H., Thallinger, G. G., Mattanovich, D., Gasser, B. & Graf, A. B. (2016) Curation of the genome annotation of Pichia pastoris (Komagataella phaffii) CBS7435 from gene level to protein function, *FEMS Yeast Res.* **16**.
6. Dikicioglu, D., Wood, V., Rutherford, K. M., McDowall, M. D. & Oliver, S. G. (2014) Improving functional annotation for industrial microbes: a case study with Pichia pastoris, *Trends in biotechnology.* **32**, 396-9.
7. Sola, A., Maaheimo, H., Ylonen, K., Ferrer, P. & Szyperski, T. (2004) Amino acid biosynthesis and metabolic flux profiling of Pichia pastoris, *European journal of biochemistry / FEBS.* **271**, 2462-70.
8. Sola, A., Jouhten, P., Maaheimo, H., Sanchez-Ferrando, F., Szyperski, T. & Ferrer, P. (2007) Metabolic flux profiling of Pichia pastoris grown on glycerol/methanol mixtures in chemostat cultures at low and high dilution rates, *Microbiology (Reading, England).* **153**, 281-90.
9. Baumann, K., Carnicer, M., Dragosits, M., Graf, A. B., Stadlmann, J., Jouhten, P., Maaheimo, H., Gasser, B., Albiol, J., Mattanovich, D. & Ferrer, P. (2010) A multi-level study of recombinant Pichia pastoris in different oxygen conditions, *BMC systems biology.* **4**, 141.
10. Celik, E., Calik, P. & Oliver, S. G. (2010) Metabolic flux analysis for recombinant protein production by Pichia pastoris using dual carbon sources: Effects of methanol feeding rate, *Biotechnology and bioengineering.* **105**, 317-29.
11. Carnicer, M., Ten Pierick, A., van Dam, J., Heijnen, J. J., Albiol, J., van Gulik, W. & Ferrer, P. (2012) Quantitative metabolomics analysis of amino acid metabolism in recombinant Pichia pastoris under different oxygen availability conditions, *Microbial cell factories.* **11**, 83.
12. Jorda, J., Jouhten, P., Camara, E., Maaheimo, H., Albiol, J. & Ferrer, P. (2012) Metabolic flux profiling of recombinant protein secreting Pichia pastoris growing on glucose:methanol mixtures, *Microbial cell factories.* **11**, 57.
13. Fazenda, M. L., Dias, J. M., Harvey, L. M., Nordon, A., Edrada-Ebel, R., Littlejohn, D. & McNeil, B. (2013) Towards better understanding of an industrial cell factory: investigating the feasibility of real-time metabolic flux analysis in Pichia pastoris, *Microbial cell factories.* **12**, 51.
14. Jorda, J., Suarez, C., Carnicer, M., ten Pierick, A., Heijnen, J. J., van Gulik, W., Ferrer, P., Albiol, J. & Wahl, A. (2013) Glucose-methanol co-utilization in Pichia pastoris studied by metabolomics and instationary (1)(3)C flux analysis, *BMC systems biology.* **7**, 17.
15. Ferrer, P. & Albiol, J. (2014) (1)(3)C-based metabolic flux analysis of recombinant Pichia pastoris, *Methods in molecular biology (Clifton, NJ).* **1191**, 291-313.
16. Jorda, J., de Jesus, S. S., Peltier, S., Ferrer, P. & Albiol, J. (2014) Metabolic flux analysis of recombinant Pichia pastoris growing on different glycerol/methanol mixtures by iterative fitting of NMR-derived (13)C-labelling data from proteinogenic amino acids, *New biotechnology.* **31**, 120-32.
17. Looser, V., Bruhlmann, B., Bumbak, F., Stenger, C., Costa, M., Camattari, A., Fotiadis, D. & Kovar, K. (2015) Cultivation strategies to enhance productivity of Pichia pastoris: A review, *Biotechnology advances.* **33**, 1177-93.
18. Maaheimo, H., Fiaux, J., Cakar, Z. P., Bailey, J. E., Sauer, U. & Szyperski, T. (2001) Central carbon metabolism of Saccharomyces cerevisiae explored by biosynthetic fractional (13)C labeling of

common amino acids, *European journal of biochemistry / FEBS.* **268**, 2464-79.
19. Fiaux, J., Cakar, Z. P., Sonderegger, M., Wuthrich, K., Szyperski, T. & Sauer, U. (2003) Metabolic-flux profiling of the yeasts Saccharomyces cerevisiae and Pichia stipitis, *Eukaryot Cell.* **2**, 170-80.
20. Papini, M., Nookaew, I., Uhlen, M. & Nielsen, J. (2012) Scheffersomyces stipitis: a comparative systems biology study with the Crabtree positive yeast Saccharomyces cerevisiae, *Microbial cell factories.* **11**, 136.
21. Hagman, A. & Piskur, J. (2015) A study on the fundamental mechanism and the evolutionary driving forces behind aerobic fermentation in yeast, *PloS one.* **10**, e0116942.
22. Neri, D., Szyperski, T., Otting, G., Senn, H. & Wuthrich, K. (1989) Stereospecific nuclear magnetic resonance assignments of the methyl groups of valine and leucine in the DNA-binding domain of the 434 repressor by biosynthetically directed fractional 13C labeling, *Biochemistry.* **28**, 7510-6.
23. Szyperski, T., Neri, D., Leiting, B., Otting, G. & Wuthrich, K. (1992) Support of 1H NMR assignments in proteins by biosynthetically directed fractional 13C-labeling, *J Biomol NMR.* **2**, 323-34.
24. Szyperski, T. (1998) 13C-NMR, MS and metabolic flux balancing in biotechnology research, *Q Rev Biophys.* **31**, 41-106.
25. Szyperski, T. (1995) Biosynthetically directed fractional 13C-labeling of proteinogenic amino acids. An efficient analytical tool to investigate intermediary metabolism, *European journal of biochemistry / FEBS.* **232**, 433-48.
26. Szyperski, T., Bailey, J. E. & Wüthrich, K. (1996) Detecting and dissecting metabolic fluxes using biosynthetic fractional <sup>13</sup>C labeling and two-dimensional NMR spectroscopy, *Trends in biotechnology.* **14**, 453-459.
27. Sauer, U., Hatzimanikatis, V., Bailey, J. E., Hochuli, M., Szyperski, T. & Wuthrich, K. (1997) Metabolic fluxes in riboflavin-producing Bacillus subtilis, *Nat Biotechnol.* **15**, 448-52.
28. Sauer, U., Lasko, D. R., Fiaux, J., Hochuli, M., Glaser, R., Szyperski, T., Wuthrich, K. & Bailey, J. E. (1999) Metabolic flux ratio analysis of genetic and environmental modulations of Escherichia coli central carbon metabolism, *J Bacteriol.* **181**, 6679-88.
29. Szyperski, T., Glaser, R. W., Hochuli, M., Fiaux, J., Sauer, U., Bailey, J. E. & Wuthrich, K. (1999) Bioreaction network topology and metabolic flux ratio analysis by biosynthetic fractional 13C labeling and two-dimensional NMR spectroscopy, *Metab Eng.* **1**, 189-97.
30. Canonaco, F., Hess, T. A., Heri, S., Wang, T., Szyperski, T. & Sauer, U. (2001) Metabolic flux response to phosphoglucose isomerase knock-out in Escherichia coli and impact of overexpression of the soluble transhydrogenase UdhA, *FEMS Microbiol Lett.* **204**, 247-52.
31. Frey, A. D., Fiaux, J., Szyperski, T., Wuthrich, K., Bailey, J. E. & Kallio, P. T. (2001) Dissection of central carbon metabolism of hemoglobin-expressing Escherichia coli by 13C nuclear magnetic resonance flux distribution analysis in microaerobic bioprocesses, *Appl Environ Microbiol.* **67**, 680-7.
32. Dauner, M., Sonderegger, M., Hochuli, M., Szyperski, T., Wuthrich, K., Hohmann, H. P., Sauer, U. & Bailey, J. E. (2002) Intracellular carbon fluxes in riboflavin-producing Bacillus subtilis during growth on two-carbon substrate mixtures, *Appl Environ Microbiol.* **68**, 1760-71.
33. Emmerling, M., Dauner, M., Ponti, A., Fiaux, J., Hochuli, M., Szyperski, T., Wuthrich, K., Bailey, J. E. & Sauer, U. (2002) Metabolic flux responses to pyruvate kinase knockout in Escherichia coli, *J Bacteriol.* **184**, 152-64.
34. Zamboni, N., Maaheimo, H., Szyperski, T., Hohmann, H. P. & Sauer, U. (2004) The phosphoenolpyruvate carboxykinase also catalyzes C3 carboxylation at the interface of glycolysis and the TCA cycle of Bacillus subtilis, *Metab Eng.* **6**, 277-84.
35. Antoniewicz, M. R. (2013) 13C metabolic flux analysis: optimal design of isotopic labeling experiments, *Current opinion in biotechnology.* **24**, 1116-21.
36. Jouhten, P., Rintala, E., Huuskonen, A., Tamminen, A., Toivari, M., Wiebe, M., Ruohonen, L., Penttila, M. & Maaheimo, H. (2008) Oxygen dependence of metabolic fluxes and energy generation of Saccharomyces cerevisiae CEN.PK113-1A, *BMC systems biology.* **2**, 60.
37. Jouhten, P., Pitkanen, E., Pakula, T., Saloheimo, M., Penttila, M. & Maaheimo, H. (2009) 13C-

metabolic flux ratio and novel carbon path analyses confirmed that Trichoderma reesei uses primarily the respirative pathway also on the preferred carbon source glucose, *BMC systems biology.* **3**, 104.
38. Sriram, G., Fulton, D. B., Iyer, V. V., Peterson, J. M., Zhou, R., Westgate, M. E., Spalding, M. H. & Shanks, J. V. (2004) Quantification of compartmented metabolic fluxes in developing soybean embryos by employing biosynthetically directed fractional (13)C labeling, two-dimensional [(13)C, (1)H] nuclear magnetic resonance, and comprehensive isotopomer balancing, *Plant Physiol.* **136**, 3043-57.
39. Hochuli, M., Patzelt, H., Oesterhelt, D., Wuthrich, K. & Szyperski, T. (1999) Amino acid biosynthesis in the halophilic archaeon Haloarcula hispanica, *J Bacteriol.* **181**, 3226-37.
40. Chung, B. K., Lakshmanan, M., Klement, M., Ching, C. B. & Lee, D. Y. (2013) Metabolic reconstruction and flux analysis of industrial Pichia yeasts, *Applied microbiology and biotechnology.* **97**, 1865-73.
41. Costenoble, R., Picotti, P., Reiter, L., Stallmach, R., Heinemann, M., Sauer, U. & Aebersold, R. (2011) Comprehensive quantitative analysis of central carbon and amino-acid metabolism in Saccharomyces cerevisiae under multiple conditions by targeted proteomics, *Molecular systems biology.* **7**, 464.
42. Forster, J., Halbfeld, C., Zimmermann, M. & Blank, L. M. (2014) A blueprint of the amino acid biosynthesis network of hemiascomycetes, *FEMS Yeast Res.* **14**, 1090-100.
43. Palmieri, F. & Pierri, C. L. (2010) Mitochondrial metabolite transport, *Essays in biochemistry.* **47**, 37-52.
44. Kohlhaw, G. B. (2003) Leucine biosynthesis in fungi: entering metabolism through the back door, *Microbiology and molecular biology reviews : MMBR.* **67**, 1-15, table of contents.
45. Laroche, Y., Storme, V., De Meutter, J., Messens, J. & Lauwereys, M. (1994) High-level secretion and very efficient isotopic labeling of tick anticoagulant peptide (TAP) expressed in the methylotrophic yeast, Pichia pastoris, *Bio/technology (Nature Publishing Company).* **12**, 1119-24.
46. Wood, M. J. & Komives, E. A. (1999) Production of large quantities of isotopically labeled protein in Pichia pastoris by fermentation, *J Biomol NMR.* **13**, 149-59.
47. Morgan, W. D., Kragt, A. & Feeney, J. (2000) Expression of deuterium-isotope-labelled protein in the yeast pichia pastoris for NMR studies, *J Biomol NMR.* **17**, 337-47.
48. van den Burg, H. A., de Wit, P. J. & Vervoort, J. (2001) Efficient 13C/15N double labeling of the avirulence protein AVR4 in a methanol-utilizing strain (Mut+) of Pichia pastoris, *J Biomol NMR.* **20**, 251-61.
49. Pickford, A. R. & O'Leary, J. M. (2004) Isotopic labeling of recombinant proteins from the methylotrophic yeast Pichia pastoris, *Methods in molecular biology (Clifton, NJ).* **278**, 17-33.
50. Huang, Y., Zhang, Y., Wu, Y., Wang, J., Liu, X., Dai, L., Wang, L., Yu, M. & Mo, W. (2012) Expression, purification, and mass spectrometric analysis of 15N, 13C-labeled RGD-hirudin, expressed in Pichia pastoris, for NMR studies, *PloS one.* **7**, e42207.
51. McCommis, K. S. & Finck, B. N. (2015) Mitochondrial pyruvate transport: a historical perspective and future research directions, *The Biochemical journal.* **466**, 443-54.
52. Rosenzweig, R. & Kay, L. E. (2014) Bringing dynamic molecular machines into focus by methyl-TROSY NMR, *Annu Rev Biochem.* **83**, 291-315.
53. Tugarinov, V., Kanelis, V. & Kay, L. E. (2006) Isotope labeling strategies for the study of high-molecular-weight proteins by solution NMR spectroscopy, *Nat Protoc.* **1**, 749-54.
54. Miyazawa-Onami, M., Takeuchi, K., Takano, T., Sugiki, T., Shimada, I. & Takahashi, H. (2013) Perdeuteration and methyl-selective (1)H, (13)C-labeling by using a Kluyveromyces lactis expression system, *J Biomol NMR.* **57**, 297-304.
55. Clark, L., Zahm, J. A., Ali, R., Kukula, M., Bian, L., Patrie, S. M., Gardner, K. H., Rosen, M. K. & Rosenbaum, D. M. (2015) Methyl labeling and TROSY NMR spectroscopy of proteins expressed in the eukaryote Pichia pastoris, *J Biomol NMR.* **62**, 239-45.
56. Nie, Y., Huang, M., Lu, J., Qian, J., Lin, W., Chu, J., Zhuang, Y. & Zhang, S. (2014) Impacts of high

beta-galactosidase expression on central metabolism of recombinant Pichia pastoris GS115 using glucose as sole carbon source via (13)C metabolic flux analysis, *J Biotechnol.* **187**, 124-34.
57. Hazelwood, L. A., Daran, J. M., van Maris, A. J., Pronk, J. T. & Dickinson, J. R. (2008) The Ehrlich pathway for fusel alcohol production: a century of research on Saccharomyces cerevisiae metabolism, *Appl Environ Microbiol.* **74**, 2259-66.
58. Crepin, L., Truong, N. M., Bloem, A., Sanchez, I., Dequin, S. & Camarasa, C. (2017) Management of Multiple Nitrogen Sources during Wine Fermentation by Saccharomyces cerevisiae, *Appl Environ Microbiol.* **83**.
59. Wiechert, W. & Noh, K. (2013) Isotopically non-stationary metabolic flux analysis: complex yet highly informative, *Current opinion in biotechnology.* **24**, 979-86.
60. Bodenhausen, G. & Ruben, D. J. (1980) Natural abundance nitrogen-15 NMR by enhanced heteronuclear spectroscopy, *Chemical Physics Letters.* **69**, 185-189.
61. Delaglio, F., Grzesiek, S., Vuister, G. W., Zhu, G., Pfeifer, J. & Bax, A. D. (1995) NMRPipe: a multidimensional spectral processing system based on UNIX pipes, *Journal of biomolecular NMR.* **6**, 277-293.

**Table 1.** Carbon sources for aerobic batch cultures of *Pichia pastoris* strain GS115.

| | |
|---|---|
| Set 1: 6 h of exponential growth | |
| 5 g/L **g**lucose | G-1 |
| 5 g/L **g**lucose, 0.1 g/L α-K**B**, 0.1 g/L α-K**I**V | GBI-1 |
| 5 g/L **g**lucose, 0.2 g/L α-K**B**, 0.2 g/L α-K**I**V | GBI-2 |
| 5 g/L **g**lucose, 0.5 g/L α-K**B**, 0.5 g/L α-K**I**V | GBI-3 |
| 5 g/L **g**lucose, 1.0 g/L α-K**B**, 1.0 g/L α-K**I**V | GBI-4 |
| Set 2: 7 h of exponential growth | |
| 5 g/L **g**lucose | G-2 |
| 5 g/L **g**lucose, 0.5 g/L **V**al | GV-2 |
| 5 g/L **g**lucose, 0.5 g/L α-K**B** | GB-2 |
| Set 3: 15 h until stationary growth is reached | |
| 5 g/L **g**lucose | G-3 |
| 5 g/L **g**lucose, 0.5 g/L **V**al | GV-3 |
| 5 g/L **g**lucose, 0.5 g/L α-K**B** | GB-3 |

**Table 2.** Flux ratios during exponential growth of *P. pastoris, P. stipitis and S. cerevisiae in* aerobic batch cultures (ub and lb denote upper and lower bounds, and TK and TA represent transketolase and transaldolase, respectively).

| Metabolites[a] | Fraction of total pool (%) | | | |
|---|---|---|---|---|
| | *P.pastoris* [b] [this study] | *P. stipitis* [19] | *S. cerevisiae* [19] | *P. pastoris*[c] [56] |
| Cytosolic | | | | |
| *PEP* from PPP through at least one transketolase reaction (ub) | **36/** *33*-**34** | 57± 9 | 0-4 | 27 |
| *R5P* from glucose (lb) | **44/** *44*-**48** | 43± 2 | 32± 2 | 56 |
| *R5P* from G3P and S7P (TK reaction) | **56/ 51**-*56* | 57± 2 | 68± 2 | 44 |
| *R5P* from E4P (TK and TA reactions) | **25/ 22**-*24* | 35± 2 | 10± 2 | - |
| *E4P* from F6P (lb) | **0/ 0**-*0* | 9± 6 | 15± 4 | 43 |
| *PEP* from cyt-OAA (PEP carboxykinase reaction) | **0/ 0**-*0* | 0-5 | - | 6 |
| *cyt-OAA* from cyt-PYR | **71/ 74**-*75* | 41± 3 | 88-100 | - |
| *cyt-OAA* reversibly converted to fumarate | **0/ 0**-*0* | 24± 10 | 0-4 | - |
| Mitochondrial | | | | - |
| *mt-PYR* from malate | **0/ 0**-*0* | 0-6 | 25-30 | - |
| *mt-OAA* from PEP (anaplerotic supply of TCA cycle) | **58/ 59**-*61* | 36± 2 | 76± 4 | 45 |
| *mt-OAA* reversibly converted to fumarate | **55/** *48*-**52** | 58± 12 | 35± 4 | - |
| *Ser* from Gly and C1 unit | **21/***17*-**19** | 17± 2 | 19± 2 | - |
| *Gly* from $CO_2$ | **4/5**-7 | 0-6 | 4±3 | - |

[a] Metabolite names are indicated in *italics* and define a metabolite pool being associated with a specific biosynthetic origin. The flux ratios provide the fraction of the total pool of the metabolite arising from this specific origin. [b] Flux ratios, or bounds thereof, were calculated with equations provided in [7, 18, 25, 27, 36]. Those shown in the left-most column are from this study: the left ratio in this column was obtained from culture G-1 (Table 1) and the range of ratios on the right in this column was obtained from culture G-2 (with one ratio obtained from 600 MHz spectra and one form 850 MHz spectra). The ratio obtained with 850 MHz spectra is indicated in *italics* (and not in bold) [c] Calculated from net fluxes of an MS based metabolic flux balancing study. The media contained 5 g/L glucose in all cases, except for the study of Nie *et al.* [56] in which the medium contained 10 g/L.

**Table 3.** Flux ratios during exponential growth of *P. pastoris* in aerobic batch cultures with glucose (G-2), glucose and Val (GV-2), or glucose and α-KB (GB-2) as carbon sources (ub and lb denote upper and lower bounds, respectively). For culture G-2 (Table 1), the ratios obtained from 600 MHz spectra are shown (see Table 2 and footnotes).

| Metabolites | Fraction of total pool (%) | | |
|---|---|---|---|
| | G-2 | GV-2 | GB-2 |
| Cytosolic | | | |
| *PEP* from PPP through at least one transketolase reaction (ub) | 34 | 31 | 36 |
| *R5P* from glucose (lb) | 48 | 48 | 47 |
| *R5P* from G3P and S7P (TK reaction) | 51 | 51 | 52 |
| *R5P* from E4P (TK and TA reactions) | 22 | 23 | 22 |
| *E4P* from F6P (lb) | 0 | 0 | 0 |
| *PEP* from cyt-OAA (PEP carboxykinase reaction) | 0 | 0 | 0 |
| *cyt-OAA* from cyt-PYR | 74 | 79 | 72 |
| *cyt-OAA* reversibly converted to fumarate | 0 | 0 | 0 |
| Mitochondrial | | | |
| *mt-PYR* from malate | 0 | 0 | 0 |
| *mt-OAA* from PEP (anaplerotic supply of TCA cycle) | 59 | 57 | 56 |
| *mt-OAA* reversibly converted to fumarate | 52 | 51 | 50 |
| *Ser* from Gly and C1 unit | 19 | 21 | 20 |
| *Gly* from $CO_2$ | 5 | 7 | 4 |

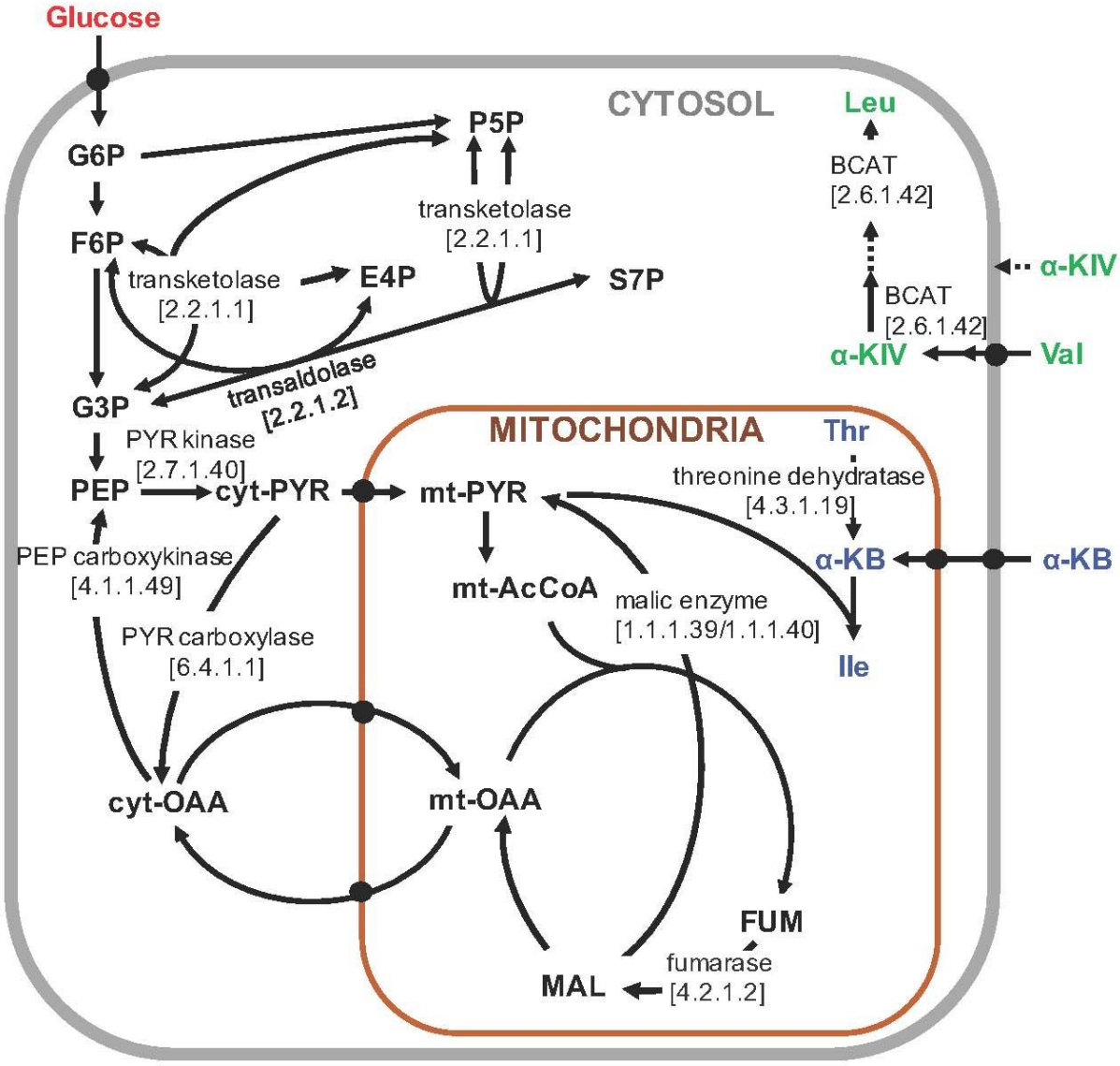


**Fig. 1.** Biochemical reaction and metabolite transporter network of *P. pastoris*. Metabolites and reactions of central carbon metabolism are shown in black, those associated with Val and Leu biosynthesis are in green, and those for Ile biosynthesis are in blue. Transporter systems are represented by black dots (for glucose: high-affinity glucose transporter, OAA: mitochondrial inner membrane transporter, PYR and α-KB: mitochondrial pyruvate carrier, Val: general amino acid permease; note that the present study indicates that *P. pastoris* does not feature a suitable transporter for *α*-KIV). The arrows indicate reaction directionality. Enzymes referred to in the text are indicated along with their EC numbers. For clarity, the reactions and enzymes associated with C1 metabolism are not shown. Abbreviations: PEP, phosphoenolpyruvate; PYR, pyruvate; OAA, oxaloacetate; AcCoA, Acetyl-Coenzyme A; FUM, fumarate; MAL, malate; α-KB, α-ketobutyrate; α-KIV, α-ketoisovalerate; G6P, glucose 6-phosphate; F6P, fructose-6-phosphate; G3P, glyceraldehyde-3-phosphate; X5P, xylulose-5-phosphate; E4P, erythrose-4-phosphate; Val, valine; Thr, threonine; Ile, isoleucine; Leu, leucine.

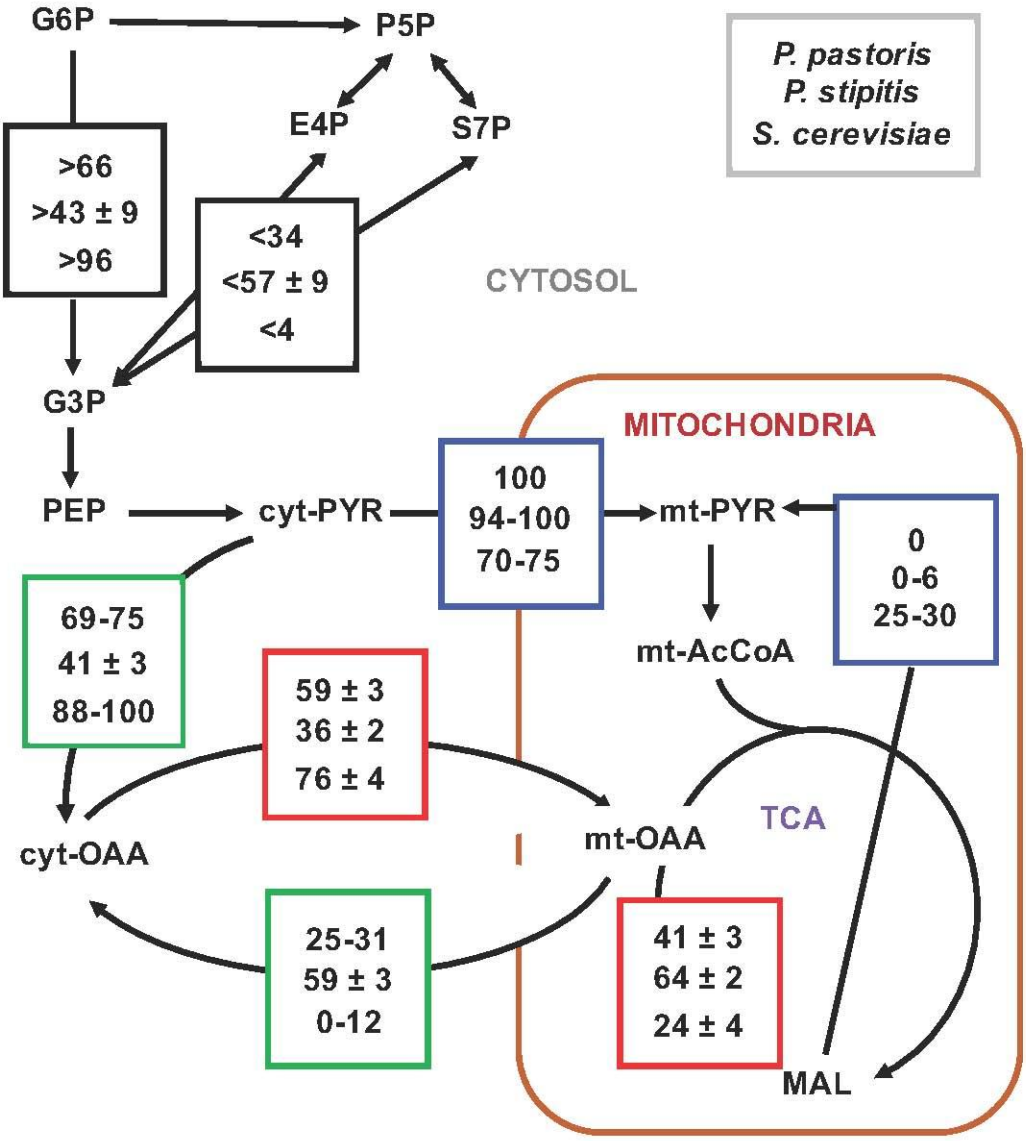


**Fig. 2.** Comparison of metabolic flux ratios obtained for *P. pastoris* (top values, this study), *P. stipitis* (middle values, [19]) and *S. cerevisiae* (bottom values,[19]) for cells growing exponentially in aerobic batch cultures containing glucose (5 g/L) as the sole carbon source. Boxes of the same color converge to the same metabolite.

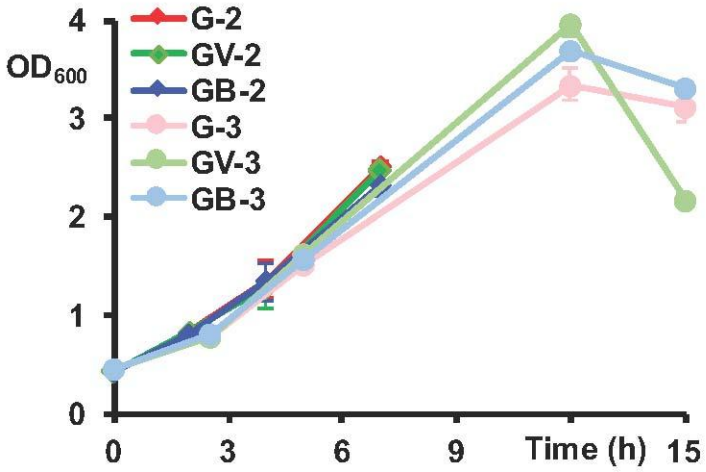


G: glucose; GV: glucose and Val; GB: glucose and α-KB

**Fig. 3.** Cell growth curves for set 2 and set 3 cultures (Table 1). As indicated below the plot, G-2 and G-3 media contain glucose only, GV-2 and GV-3 media contain glucose and Val, and GB-2 and GB-3 media contain glucose and α-KB. The color coding is: dark red for G-2, light red for G-3, dark green for GV-2, light green for GV-3, dark blue for GB-2 and light blue for GB-3.

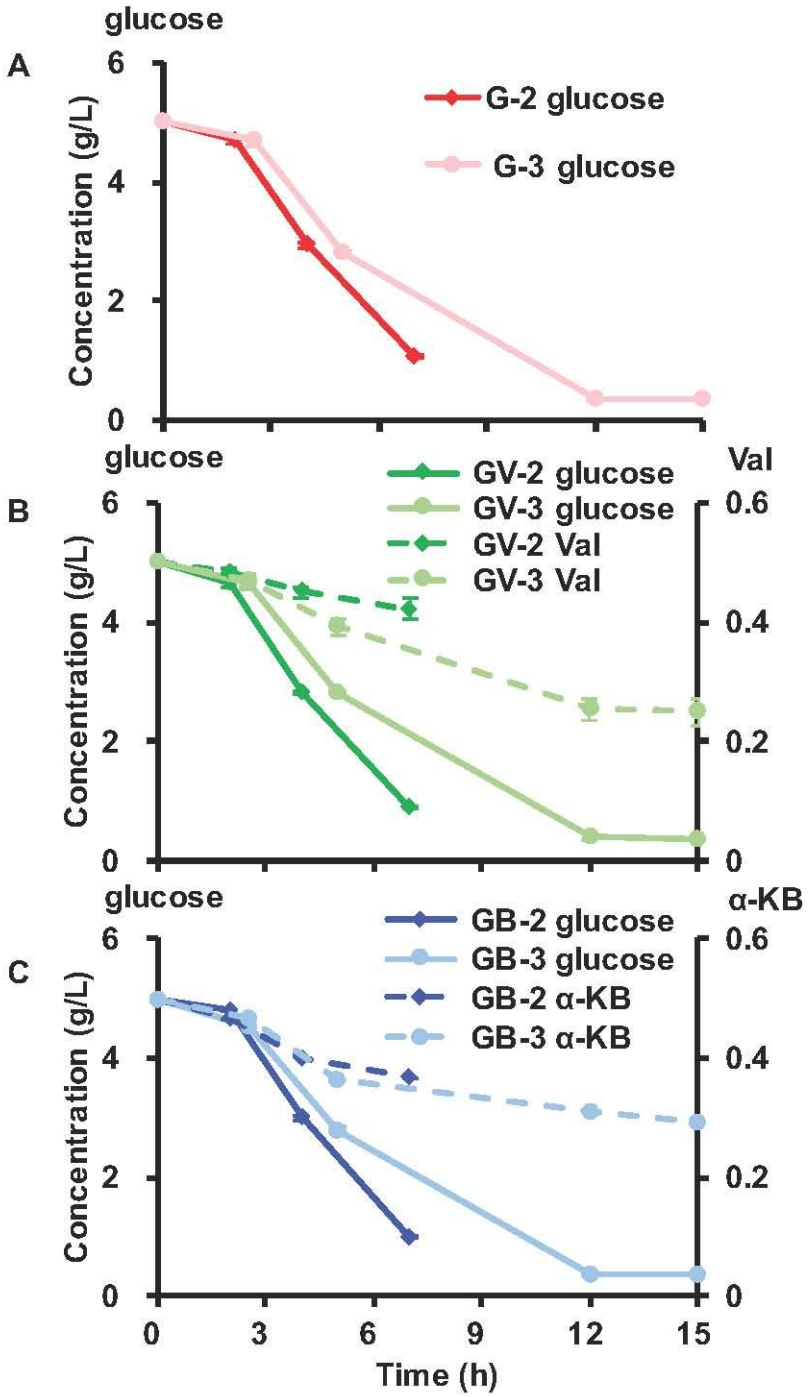


**Fig. 4.** Concentrations of carbon source metabolites *versus* time in set 2 and 3 cultures (A) G-2 and G-3 (glucose only), (B) GV-2 and GV-3 (glucose and Val), and (C) GB-2 and GB-3 (glucose and α-KB). The color coding is as in Fig. 3: dark red for G-2, light red for G-3, dark green for GV-2, light green for GV-3, dark blue for GB-2 and light blue for GB-3.

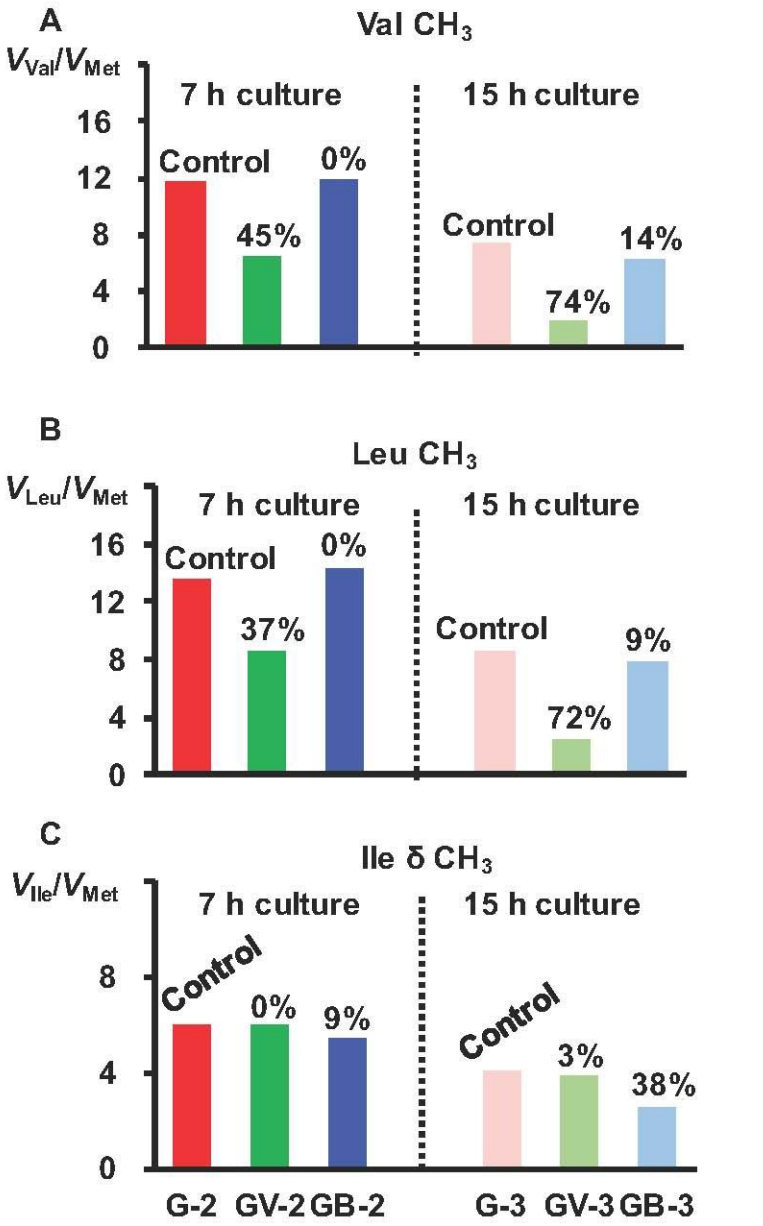


**Fig. 5.** Bar plots of the normalized volumes of methyl group signals measured in HSQC spectra (see text) recorded for set 2 and set 3 cultures (Table 1). G-2 and G-3 media contain glucose only, GV-2 and GV-3 media contain glucose and Val, and GB-2 and GB-3 media contain glucose and α-KB. (A) average of $\gamma^1$- and$\gamma^2$-$CH_3$ of Val, (B) average of $\delta^1$- and $\delta^2$-$CH_3$ of Leu, and (C) $\delta^1$-$CH_3$ of Ile. The degrees of $^{13}$C-unlabeling are indicated above the bars for GV-2, GV-3, GB-2 and GB-3. The color coding of the bars follows Figs. 3 and 4 and is: dark red for G-2, light red for G-3, dark green for GV-2, light green for GV-3, dark blue for GB-2 and light blue for GB-3.

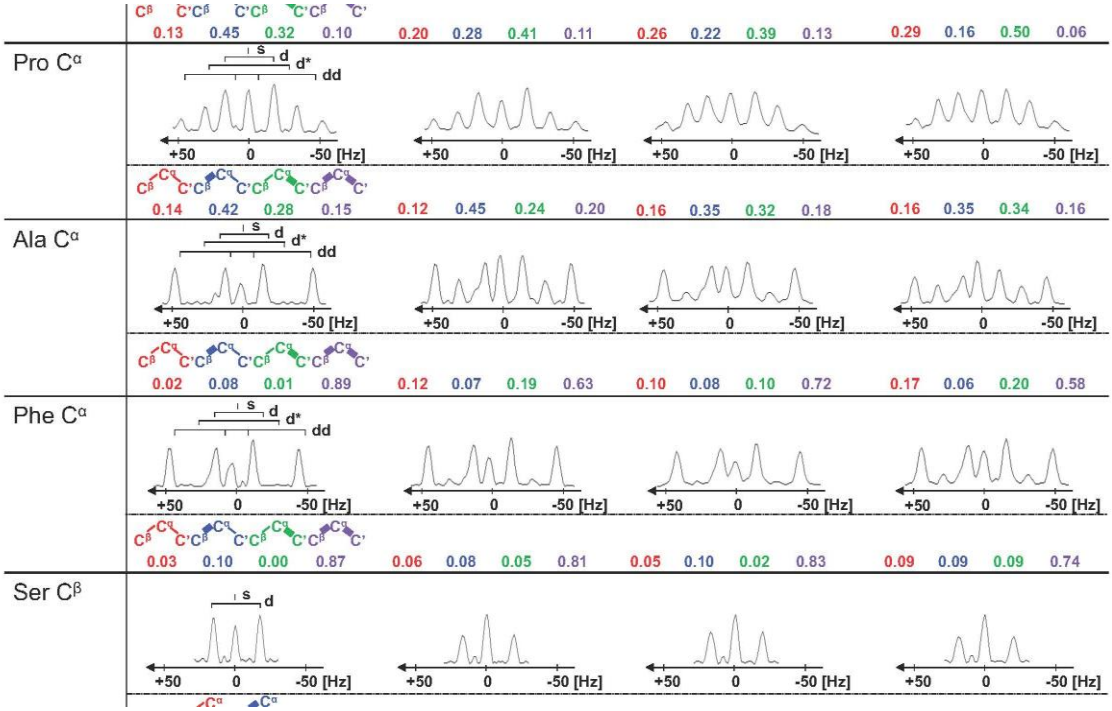


**Fig. 6.** $^{13}C$–$^{13}C$ scalar coupling fine structures taken along $\omega_1(^{13}C)$ of HSQC spectra recorded for cultures G-2, G-3, GV-3 and GB-3 (Table 1). G-2 and G-3 media contain glucose only, GV-2 and GV-3 media contain glucose and Val, and GB-2 and GB-3 media contain glucose and α-KB. As indicated in the left-most column for G-2, the fine structures observed for the α-carbons consist of a singlet (s) representing the $^{12}C'$-$^{\mathbf{13}}\mathbf{C}^{\boldsymbol{\alpha}}$-$^{12}C^{\beta}$ isotopomer, a doublet (d) arising from $^{12}C'$-$^{\mathbf{13}}\mathbf{C}^{\boldsymbol{\alpha}}$-$^{\mathbf{13}}\mathbf{C}^{\boldsymbol{\beta}}$, a second doublet (d*) arising from $^{\mathbf{13}}\mathbf{C}'$-$^{\mathbf{13}}\mathbf{C}^{\boldsymbol{\alpha}}$-$^{12}C^{\beta}$, and a doublet of doublets arising from $^{\mathbf{13}}\mathbf{C}'$-$^{\mathbf{13}}\mathbf{C}^{\boldsymbol{\alpha}}$-$^{\mathbf{13}}\mathbf{C}^{\boldsymbol{\beta}}$. The β-carbon of Ser consists only of a singlet (s) and a doublet (d) arising from $^{13}C^{\alpha}$-$^{\mathbf{13}}\mathbf{C}^{\boldsymbol{\beta}}$ and $^{\mathbf{13}}\mathbf{C}^{\boldsymbol{\alpha}}$-$^{\mathbf{13}}\mathbf{C}^{\boldsymbol{\beta}}$, respectively. The intact carbon fragments are shown in different colors below the cross sections: thick bonds indicate that the connected carbons originate from the same source molecule of glucose. The corresponding *f* values (Tables S2, S4, S7, S9) are provided below the intact carbon fragments in their respective colors. For G-3, GV-3 and GB-3, only the *f* values are displayed for clarity. Comparison of the cross sections and *f* values reveal changes of metabolic regulation in the stationary phase (see text).